Nonlinear adaptive backstepping controller design for controlling bidirectional power flow of BESSs in DC microgrids

DOI: http://dx.doi.org/10.1109/IAS.2016.7731875

Nonlinear Adaptive Backstepping Controller Design for Controlling Bidirectional Power Flow of BESSs in DC Microgrids

T. K. Roy, *Student Member, IEEE*, M. A. Mahmud, *Member, IEEE*, A. M. T. Oo, *Member, IEEE*, M. E. Haque, *Senior Member, IEEE*, K. M. Muttaqi, *Senior Member, IEEE*, and N. Mendis, *Member, IEEE*

***Abstract*—In this paper, a nonlinear adaptive backstepping controller is designed to control the bidirectional power flow (charging/discharging) of battery energy storage systems (BESSs) in a DC microgrid under different operating conditions. The controller is designed in such a manner that the BESSs can store the excess energy from the renewable energy sources (RESs) in a DC microgrid after satisfying the load demand and also feeding back the stored energy to the load when RESs are no sufficient. The proposed controller is also designed to maintain a constant voltage at the DC bus, where all components of DC microgrids are connected, while controlling the power flow of BESSs. This paper considers solar photovoltaic (PV) systems as the RES whereas a diesel generator equipped with a rectifier is used as a backup supply to maintain the continuity of power supply in the case of emergency situations. The controller is designed recursively based on the Lyapunov control theory where all parameters within the model of BESSs are assumed as unknown. These unknown parameters are then estimated through the adaptation laws and whose stability is ensured by formulating suitable control Lyapunov functions (CLFs) at different stages of the design process. Moreover, a scheme is also presented to monitor the state of charge (SOC) of the BESS. Finally, the performance of the proposed controller is verified on a test DC microgrid under various operating conditions. The proposed controller ensures the DC bus voltage regulation within the acceptable limits under different operating conditions.**

***Index Terms*—Adaptive backstepping controller, battery energy storage system, control Lyapunov function, DC microgrid, renewable energy sources.**

I. Introduction

THE INTEGRATION of renewable energy sources (RESs) has been significantly increased over the past few decades. The growth rate of integrating RESs is promising to solve the energy problems and environmental pollution such as greenhouse gas emission. It is well known that if the integration of large-scale RESs especially solar photovoltaic (PV) systems into an existing utility grid (which are far away from the consumers) is not a cost-effective solutions and there are also several technical challenges such as voltage stability, frequency stability, and power quality [1]. Microgrids which allow to connect the RESs close to the consumers can be used as a cost-effective solution to these problems [2]–[5].

Microgrids usually have the capability to generate their own power to meet the load requirements. Thus, a microgrid be operated in an islanded mode if it has the ability to generate its own power during the emergency condition e.g., when the battery energy storage systems (BESSs) are fully discharged and no power is available from the RESs. Usually, diesel generators are used as standby supply to meet the load demands during the emergency conditions. These types of microgrids are used for rural areas where the frequent delivery of conventional fossil fuel is more expensive. However, a microgrid can be connected to the main grid if there exists such provisions or there are no standby diesel generators. Thus, a microgrids can be operated either in islanded or standalone mode. The loads in microgrids can either be AC or DC as well as combination of both AC and DC. Most of the components in microgrids are primarily based on the DC voltage, e.g., the output voltage of solar PV systems is DC and similarly, BESSs store DC power. Thus, the operation of DC microgrids will be more economical and technically robust than AC microgrids [6]–[12].

There are several benefits of employing DC microgrids. If loads are supplied directly with DC power, the efficiency of the system becomes higher owing to the reduction of conversion losses from sources to loads [13]. Nonetheless DC microgrids can overcome some limitations associated with AC microgrids such as frequency synchronization, control of reactive power flow, and power quality issues [6]. Recently, the deployments of DC microgrids are resurging due to the utilization of RESs based on DC output power and their inherent advantage for DC loads in commercial, and residential applications. A low voltage DC microgrid is proposed in [1] to supply the power in a residential complex where the super capacitor is used as the main power supply. A solar PV based standalone DC microgrid for supplying small-scale residential DC loads as proposed in [14] has achieved a great deal of attention owing to the distinctive advantages of solar PV systems.

Despite of several advantages as mentioned above, there are several challenges in the operation of DC microgrids. Among these challenges, the maintenance of power balance for continuously changing load conditions and intermittent characteristics of solar PV systems are considered to be critical. The stable and reliable operation of DC microgrids depend on their ability to maintain the power balance between the sources and loads under changing and uncertain operating conditions. In such situations, energy storage systems (ESSs) play a vital role in maintaining the energy balance of DC microgrids [15]. Most commonly used ESSs in a microgrid are batteries, super capacitors, and hydrogen storage for fuel cells, etc. among which BESSs are the mostly preferred option.

BESSs are responsible for minimizing the mismatch between

T. K. Roy, M. A. Mahmud, and A. M. T. Oo are with the School of Engineering, Deakin University, Waurn Ponds, VIC 3216, Australia. Email: (tkroy, apel.mahmud, and aman.m)@deakin.edu.au

K. M. Muttaqi is with the School of Electrical, Computer and Telecommunications Engineering, University of Wollongong, NSW 2522, Australia. Email: Kashem@uow.edu.au

N. Mendis is with the Eltek Australia Pty Ltd, Port Melbourne, VIc 3207, Australia. Email: nnrm786@uowmail.edu.au

the generation and load demand due to stochastic variations of RESs as well as loads. A controlled operation of the BESS will allow to minimize the demand-generation mismatch of the microgrid system [16], [17]. Although the integration of BESSs guarantees the stability of microgrids, however, add further complexities into the system in terms of energy management and control for managing peak demands and variations in the load demands. Hence, a bidirectional control scheme is required to control the bidirectional power flow between the DC bus and BESS in a DC microgrid.

The stability of DC microgrids relies on the regulation of DC bus voltage which is mainly used to supply the loads. Thus, the control of the DC bus voltage is important as this is treated as an indicator of power balancing in DC microgrids [18]. The droop control technique is one of the most commonly used techniques for regulating DC bus voltage in microgrids. This technique detects the current or output power as the feedback factor or the deviation of the bus voltage is controlled in proportion to the output power [19], [20]. However, this is not the best solution when power electronics converters are connected to different devices such as solar PV systems, wind generators, and BESSs with different sets of state of charges (SOCs) [21], [22]. To overcome this limitation, a gain-scheduling control in aggregation with a centralized fuzzy controller has been proposed in [23] which can support to achieve good voltage regulation, power sharing, and energy balance in a DC microgrid. However, the approach as proposed in [23] uses a centralized fuzzy controller in order to modify the voltage reference for balancing the stored energy. Moreover, the controllers as presented in [19]–[23] are designed either based on the static or linearized models of BESSs whose operations are limited over a fixed set of operating points. Therefore, the wide variations of operating points cannot be tackled with these controllers.

Nonlinear controllers are independent of operating points and thus, overcome the limitations of linear controllers. In [24], [25], a nonlinear sliding mode controller (SMC) is proposed to regulate the DC bus voltage of a DC microgrid by considering bidirectional power flow. Though this SMC is less sensitive to parameter variations and external disturbances but the selection of the time-varying surface is very difficult. Moreover, the strategy as proposed in [24] only takes into account the case when the batteries are supplying power to the load and to the implementation of any charging algorithm is not presented though this is necessary for the batterys health and its prolonged life [26].

This paper proposes of an adaptive backstepping controller design technique for BESSs used in DC microgrids. The main control objective of the proposed scheme is to regulate the DC bus voltage under changing load and atmospheric conditions. The controllers are designed in such a way that the parameters of BESSs are considered as unknown and then adapted using adaptation laws. Control Lyapunov functions (CLFs) are used to analyze the stability of the whole system with the proposed control scheme. Additionally an algorithm is also proposed to monitor the remaining energy level of BESSs. The performance of the proposed controller is evaluated under different operating scenarios.

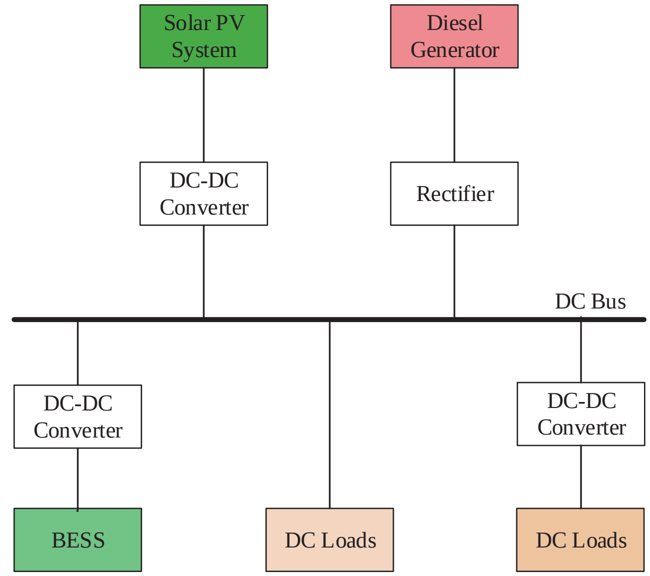

Fig. 1. DC microgrid with BESS and diesel generator

II. System Configuration, Operation Strategy, and Power Management

In the following, the configuration of the DC microgrid is discussed along with its operating strategy and power management.

A. System Configuration

The configuration of a typical solar PV-based DC microgrid which is investigated in this paper is shown in Fig. 1. It consists of a 110 V DC bus where all components of the microgrid are either connected directly or through power electronic converters. A PV source is connected to the DC bus through a DC-DC converter, the diesel generator is connected through a rectifier, a BESS is connected via a bidirectional converter, and the resistive load could be connected either directly or via DC-DC converter based is directly connected.

The primary power source within this microgrid is the solar PV system having the highest priority for supplying power. In the autonomous mode of operation, the available power from the PV unit must meet the total load demand. Otherwise, the BESS is required to supply the difference and in the case of insufficient storage, the system must undergo load shedding or need to be supplied by the diesel generator to match the generation and load demand. The BESS with a bidirectional converter can meet the responsive local load demand to maintain the healthy operation of the microgrid in case of fluctuations in the power supply from the PV unit.

B. Operation Strategy

For the satisfactory operation of the DC microgrid during the variations in solar irradiation and loads, different operating modes need to be considered in order to ensure a secure and reliable power supply. To achieve the aforementioned objective, two major operating modes are considered in this paper. The first operating mode is the power delivery mode to the loads from the renewable and BESS. In this mode, the output power of the PV system is transferred to the load and BESS as well as from the BESS to the load depending on the situations. The BESS is regulated to smooth the fluctuations of the power difference between the varying output power of the PV unit and changing DC loads to ensure that the DC voltage is maintained at the reference value. The second operating mode is the standby mode which only consists of with the standby diesel generator, the BESS, and the load. Specially, this mode will be activated when the PV power will not be available and the SOC of the BESS is less than 30%. Thus, the power can be transferred from the diesel generator to the load and BESS based on the requirement and the diesel generator can maintain the constant DC bus voltage for stable operation of the microgrid.

C. DC Voltage and Power Flow Balance

In order to evaluate the performance of the microgrid, the PV system is activated first to build the DC bus voltage as it is a good indicator of the systems operational status. A power balance constraint is that the total power generation must satisfy the total load demand. Hence, the net power (P_{net}) of the microgrid can be defined as:

$$P_{net} = P_{pv} + P_{DG} \pm P_B - P_L \tag{1}$$

where P_{pv} is the output power of the PV, P_{DG} is the diesel generator power, P_B is the BESS output power, and P_L is the power demanded by the load. However, P_{net} is always varying due to the intermittent nature of the solar PV and variation of local loads. In this situation, the BESS plays a significant role for maintaining the stability of microgrids. The BESS operates at charging and discharging modes depending on the power requirement as in (1). The dynamics of DC bus voltage in a microgrid can be formulated based on the following power balance principle:

$$CV_{dc}\frac{dV_{dc}}{dt} = P_{net} \tag{2}$$

and

$$P_{dc} = V_{dc} i_{dc} \tag{3}$$

where V_{dc} is the DC bus voltage, i_{dc} is the total current injecting into the DC bus, C is the total output capacitance for all converters. From equation (2), it can be seen that a constant DC bus voltage indicates a balanced power flow and rising or dropping DC bus voltage indicates power surplus or deficit, respectively. From equation (3), it can also be seen that it is necessary to keep the power balance at the DC bus in order to regulate the DC bus voltage. The proposed control method will help to maintain the power balance in the microgrid by controlling the bidirectional power flow of the BESS while maintain the SOC of the BESS within the safe limits. The control of BESSs requires a mathematical model which is discussed in the following section along with the problem statement.

III. BESS Modeling and Problem Statement

Batteries are electrochemical devices that store energy from other AC or DC sources for later use [27]. As stated in earlier sections, BESSs can either store or deliver energy based on the requirements of the microgrid through their control actions. The performance of the controller relies on the modeling accuracy of BESSs. BESSs exhibit highly nonlinear characteristics due to their inherent electrochemistry. In this paper, the mathematical model of BESSs is developed to facilitate the control actions for bidirectional power flow. The equivalent circuit diagram of a BESS with a bidirectional converter is shown in Fig. 2 which is used to develop the dynamical model. Based on Fig. 2, the dynamics of the BESS along with the bidirectional converter can be described by the following nonlinear state-space differential equations [16]:

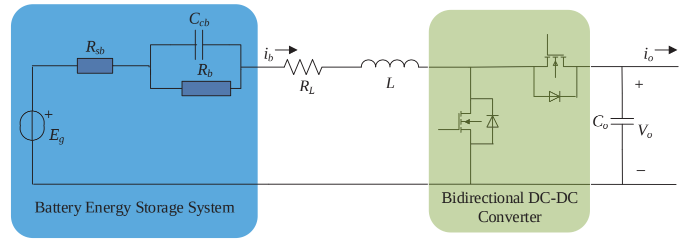

Fig. 2. BESS with bidirectional DC-DC buck-boost converter

$$\begin{aligned}
\frac{dV_{cb}}{dt} &= \frac{1}{C_{cb}}(i_b - \frac{V_{cb}}{R_b}) \\
\frac{di_b}{dt} &= \frac{1}{L}[-(R_L + R_{sb})i_b + (1-u)V_0 - V_{cb} + E_g] \\
\frac{dV_0}{dt} &= \frac{1}{C_0}[(1-u)i_b - i_0]
\end{aligned} \tag{4}$$

where the symbols have their usual meanings as in [16]. The control action of BESSs determines the proper duty cycle of the bidirectional converter in order to maintain the desired DC bus voltage while the output power of the BESS varies depending on the operating modes (charging or discharging). In practice, the parameters of BESSs are not exactly known and the variations of these parameters are sensitive to the steady-state operation. In equations (4) which represent the dynamical model of a BESS with a bidirectional converter, the parameters of the bidirectional converter (L and C_0) and the BESS (R_b and C_b) are considered as unknown as these parameters cannot be exactly known due to the presence of large magnetic flux density in the ferromagnetic core in the circuit, temperature, production materials [28] and electro-chemical reaction [15]. When these parameters are considered as unknown, it can be written as:

$$\begin{aligned}
\theta_1 &= \frac{1}{C_b} \\
\theta_2 &= \frac{1}{C_b R_b} \\
\theta_3 &= \frac{R_L + R_{sb}}{L} \\
\theta_4 &= \frac{1}{L} \\
\theta_5 &= \frac{1}{C_0}
\end{aligned} \tag{5}$$

By incorporating all these unknown parameters into the dynamical model of the BDC system as represented by equations (4), it can be written as:

$$\begin{aligned}
\dot{x}_1 &= \theta_1 x_2 - \theta_2 x_1 \\
\dot{x}_2 &= -\theta_3 x_2 + \theta_4[(1-u)x_3 - x_1 + E_g] \\
\dot{x}_3 &= \theta_5[(1-u)x_2 - i_0]
\end{aligned} \tag{6}$$

where $x_1 = V_{cb}, x_2 = i_b$, and $x_3 = V_0$, are the new states of the BDC. Based on the mathematical model as described by equations (6), the design procedure of a nonlinear adaptive backstepping controller is elaborated in the next section.

IV. Adaptive Backstepping Controller Design

The purpose of this section is to describe the design procedure of the proposed adaptive backstepping controller with an aim to control DC bus voltage while maintaining the power balance throughout the system. The design procedure of the proposed controller includes three steps as discussed in the following:

Step 1: According to the design objective, the first tracking error of the converter can be defined as:

$$e_1 = x_1 - x_{1d} \tag{7}$$

The derivative of this error can be written as:

$$\dot{e}_1 = \dot{x}_1 = \theta_1 x_2 - \theta_2 x_1 \tag{8}$$

In order to handle the unknown parameters θ_1 and θ_2 as appeared in (8); it is essential to define these parameters in term of their estimated values $\hat{\theta}_1$ and $\hat{\theta}_2$. Now the estimation errors of these parameters can be defined as $\tilde{\theta}_i = \theta_i - \hat{\theta}_i$ with $i = 1, 2$. Thus in terms of estimation error,equation (8) can be rewritten as:

$$\dot{e}_1 = (\tilde{\theta}_1 + \hat{\theta}_1)x_2 - (\tilde{\theta}_2 + \hat{\theta}_2)x_1 \tag{9}$$

In equation (9), x_2 behaves as a virtual control variable for which the CLF can be written as:

$$W_1 = \frac{1}{2}(e_1^2 + \frac{1}{\gamma_1}\tilde{\theta}_1^2 + \frac{1}{\gamma_2}\tilde{\theta}_2^2) \tag{10}$$

where γ_1 and γ_2 represent the adaptation gains which are selected in such a way that the estimation errors converge to zero. Now by inserting equation (9) into equation (10)), it can be written as:

$$\begin{aligned}\dot{W}_1 = {} & e_1(\hat{\theta}_1 x_2 - \hat{\theta}_2 x_1) - \frac{1}{\gamma_1}\tilde{\theta}_1(\dot{\hat{\theta}}_1 - \gamma_1 e_1 x_2) \\ & - \frac{1}{\gamma_2}\tilde{\theta}_2(\dot{\hat{\theta}}_2 + \gamma_2 e_1 x_1)\end{aligned} \tag{11}$$

The derivative of the CLF as represented by equation (11) should be negative semi-definite, i.e., $\dot{W}_1 \leq 0$ in order to stabilize the dynamics of first equation (6). Thus, the synthetic value of x_2 needs to be selected in such a way that it would make $\dot{W}_1 \leq 0$. In such case, the synthetic value of x_2 is chosen as follows:

$$\alpha = \frac{1}{\hat{\theta}_1}(\hat{\theta}_2 x_1 - k_1 e_1) \tag{12}$$

where k_1 is a constant which is the gain of the controller. And the influence of $\tilde{\theta}_1$ and $\tilde{\theta}_2$ from equation (11) can be eliminated by designing the following adaptation laws:

$$\begin{aligned}\dot{\hat{\theta}}_1 &= \gamma_1 e_1 x_2 \\ \dot{\hat{\theta}}_2 &= -\gamma_2 e_1 x_1\end{aligned} \tag{13}$$

However, to overcome the over-parameterization problems caused by the appearance of θ_1 and θ_2 in the subsequence steps, the adaptation laws as represented by equations (13) will not be used at this step to update $\hat{\theta}_1$ and $\hat{\theta}_2$. Instead, the following tuning functions are defined:

$$\begin{aligned}\tau_1 &= \gamma_1 e_1 x_2 \\ \tau_2 &= \gamma_2 e_1 x_1\end{aligned} \tag{14}$$

Now using the stabilizing function as represented by equation (12), the derivative of W_1 which is reflected through equation (11) can be written as:

$$\dot{W}_1 = -k_1 e_1^2 - \frac{1}{\gamma_1}\tilde{\theta}_1(\dot{\hat{\theta}}_1 - \tau_1) - \frac{1}{\gamma_2}\tilde{\theta}_2(\dot{\hat{\theta}}_2 + \tau_2) \tag{15}$$

At this point, the time derivative of α is calculated as it is essential to use in the next step and this derivative can be written as:

$$\dot{\alpha} = Ax_2\theta_1 - Ax_1\theta_2 + B \tag{16}$$

where

$$\begin{aligned}A &= \frac{\hat{\theta}_2 - k_1}{\hat{\theta}_1} \\ B &= \frac{\dot{\hat{\theta}}_2 x_1}{\hat{\theta}_1} - \frac{\dot{\hat{\theta}}_1}{\hat{\theta}_1^2}(\hat{\theta}_2 x_1 - k_1 e_1)\end{aligned}$$

Step 2: The second error variable can be defined as:

$$e_2 = x_2 - \alpha \tag{17}$$

and its derivative can be written as:

$$\begin{aligned}\dot{e}_2 = {} & -\theta_3 x_2 + \theta_4[(1-u)x_3 - x_1 + E_g] \\ & - Ax_2\theta_1 + Ax_1\theta_2 - B\end{aligned} \tag{18}$$

In terms of estimation errors, equation (18) can be rewritten as:

$$\begin{aligned}\dot{e}_2 = {} & -(\tilde{\theta}_3 + \hat{\theta}_3)x_2 + (\tilde{\theta}_4 + \hat{\theta}_4)[(1-u)x_3 - x_1 + E_g] \\ & - Ax_2(\tilde{\theta}_1 + \hat{\theta}_1) + Ax_1(\tilde{\theta}_2 + \hat{\theta}_2) - B\end{aligned} \tag{19}$$

In this case, the second CLF can be written as:

$$W_2 = W_1 + \frac{1}{2}(e_2^2 + \frac{1}{\gamma_3}\tilde{\theta}_3^2 + \frac{1}{\gamma_4}\tilde{\theta}_4^2) \tag{20}$$

Now by inserting equations (15) and (19), the derivative of W_2 can be written as:

$$\begin{aligned}\dot{W}_2 = {} & -k_1 e_1^2 + e_2[-\hat{\theta}_3 x_2 + \hat{\theta}_4((1-u)x_3 - x_1 \\ & + E_g) - Ax_2\hat{\theta}_1 + Ax_1\hat{\theta}_2 - B] - \frac{1}{\gamma_3}\tilde{\theta}_3[\dot{\hat{\theta}}_3 + e_2\gamma_3 x_2 \\ & - \frac{1}{\gamma_4}\tilde{\theta}_4[\dot{\hat{\theta}}_4 - \gamma_4 e_2((1-u)x_3 - x_1 + E_g)] - \frac{1}{\gamma_1}\tilde{\theta}_1(\dot{\hat{\theta}}_1 \\ & - \tau_1 + \gamma_1 e_2 Ax_2) - \frac{1}{\gamma_2}\tilde{\theta}_2(\dot{\hat{\theta}}_2 + \tau_2 - \gamma_2 e_2 Ax_1)\end{aligned} \tag{21}$$

Now it is essential to make $\dot{W}_2 \leq 0$ to ensures the stability of the dynamics as represented by equation (21) and this would happen if

$$\begin{aligned}& -\hat{\theta}_3 x_2 + \hat{\theta}_4((1-u)x_3 - x_1 + E_g) - Ax_2\hat{\theta}_1 \\ & + Ax_1\hat{\theta}_2 - B = -k_2 e_2\end{aligned} \tag{22}$$

Then, equation (21) reduces to

$$\begin{aligned}\dot{W}_2 = {} & -k_1 e_1^2 - k_2 e_2^2 - \frac{1}{\gamma_3}\tilde{\theta}_3(\dot{\hat{\theta}}_3 + \tau_3) - \frac{1}{\gamma_1}\tilde{\theta}_1(\dot{\hat{\theta}}_1 \\ & - \tau_{11}) - \frac{1}{\gamma_2}\tilde{\theta}_2(\dot{\hat{\theta}}_2 - \tau_{22}) - \frac{1}{\gamma_4}\tilde{\theta}_4(\dot{\hat{\theta}}_4 - \tau_4)\end{aligned} \tag{23}$$

where

$$\begin{aligned}\tau_3 &= \gamma_3 e_2 x_2 \\ \tau_4 &= e_2\gamma_4((1-u)x_3 - x_1 + E_g) \\ \tau_{11} &= \tau_1 - \gamma_1 e_2 x_2 A \\ \tau_{22} &= \tau_2 - \gamma_2 e_2 x_1 A\end{aligned}$$

The derivation of control law along with the stability and robustness analysis of the whole system is shown in the following step.

Step 3: Since $-\hat{\theta}_3x_2+\hat{\theta}_4((1-u)x_3-x_1+E_g)-Ax_2\hat{\theta}_1+Ax_1\hat{\theta}_2-B$ and $-k_2e_2$ may not be equal so the final error based on equation (22) can be obtained as follows:

$$\begin{aligned} e_3 = & -\hat{\theta}_3x_2+\hat{\theta}_4((1-u)x_3-x_1+E_g)-Ax_2\hat{\theta}_1 \\ & +Ax_1\hat{\theta}_2-B+k_2e_2 \end{aligned} \tag{24}$$

whose derivative can be written as:

$$\dot{e}_3 = A_1(\theta_1x_2-\theta_2x_1)-B_1\theta_3x_2+C_1\theta_4+D_1\theta_5+E_1 \tag{25}$$

where

$$\begin{aligned} A_1 &= A\hat{\theta}_2+\frac{\dot{\hat{\theta}}_2}{\hat{\theta}_1}-\frac{\dot{\hat{\theta}}_1}{\hat{\theta}_1^2}(\hat{\theta}_2-k_1)-\hat{\theta}_4 \\ B_1 &= -(A\hat{\theta}_1-\hat{\theta}_3) \\ C_1 &= B_1[(1-u)x_3-x_1+E_g] \\ D_1 &= (1-u)\hat{\theta}_1[(1-u)x_2-i_0] \\ E_1 &= \dot{\hat{\theta}}_3((1-u)x_3-(R_L+R_{sb})x_2-x_1+E_g)+\frac{1}{\hat{\theta}_1}\ddot{\hat{\theta}}_2x_1 \\ & -\frac{2}{\hat{\theta}_1^2}\dot{\hat{\theta}}_1\dot{\hat{\theta}}_2x_1+(\hat{\theta}_2x_1-k_1e_1)\left(\frac{2}{\hat{\theta}_1^3}\dot{\hat{\theta}}_1^2-\frac{1}{\hat{\theta}_1^2}\ddot{\hat{\theta}}_2\right) \end{aligned}$$

By incorporating the estimation errors, equation (25) can be rewritten as:

$$\begin{aligned} \dot{e}_3 = & (\tilde{\theta}_1+\hat{\theta}_1)A_1x_2-A_1(\tilde{\theta}_2+\hat{\theta}_2)x_1-B_1x_2(\tilde{\theta}_3+\hat{\theta}_3) \\ & +C_1(\tilde{\theta}_4+\hat{\theta}_4)+D_1(\tilde{\theta}_5+\hat{\theta}_5)-\dot{u}\hat{\theta}_4x_3 \end{aligned} \tag{26}$$

At this point, the CLF is written as:

$$W_3 = W_2+\frac{1}{2}(e_3^2+\frac{1}{\gamma_5}\tilde{\theta}_5^2) \tag{27}$$

By substituting the values of $\dot{W}_2$ and $\dot{e}_3$, the derivative of W_3 can be written as:

$$\begin{aligned} \dot{W}_3 = & -k_1e_1^2-k_2e_2^2+e_3[A_1(\hat{\theta}_1x_2-\hat{\theta}_2x_1)-B_1\hat{\theta}_3x_2 \\ & +C_1\hat{\theta}_4+E_1+D_1\hat{\theta}_5-\dot{u}\hat{\theta}_4x_3]-\frac{\tilde{\theta}_1}{\gamma_1}(\dot{\theta}_1-\tau_{11}-\gamma_1e_3 \\ & A_1x_2)-\frac{\tilde{\theta}_2}{\gamma_2}(\dot{\theta}_2-\tau_{22}+\gamma_2e_3A_1x_1)-\frac{\tilde{\theta}_3}{\gamma_3}(\dot{\theta}_3+\tau_3 \\ & +\gamma_3e_3B_1x_2)-\frac{\tilde{\theta}_4}{\gamma_4}(\dot{\theta}_4-\tau_4-\gamma_4e_3C_1) \\ & -\frac{\tilde{\theta}_5}{\gamma_5}(\dot{\theta}_5-\gamma_5e_3D_1) \end{aligned} \tag{28}$$

The adaptive control law for controlling the duty cycle of the BDC can be chosen as:

$$\begin{aligned} \dot{u} = & \frac{1}{\hat{\theta}_4x_3}(A_1(\hat{\theta}_1x_2-\hat{\theta}_2x_1)-B_1\hat{\theta}_3x_2+C_1\hat{\theta}_4 \\ & +D_1\hat{\theta}_5+E_1+k_3e_3) \end{aligned} \tag{29}$$

And in order to eliminate the influence of $\tilde{\theta}_1$, $\tilde{\theta}_2$, $\tilde{\theta}_3$, $\tilde{\theta}_4$, and $\tilde{\theta}_5$ in $\dot{W}_3$; the following adaptation laws can be chosen:

$$\begin{aligned} \dot{\theta}_1 &= \tau_{11}+\gamma_1e_3A_1x_2 \\ \dot{\theta}_2 &= \tau_{22}-\gamma_2e_3A_1x_1 \\ \dot{\theta}_3 &= -(\tau_3+\gamma_3e_3B_1x_2) \\ \dot{\theta}_4 &= \tau_4+\gamma_4e_3C_1 \\ \dot{\theta}_5 &= \gamma_5e_3D_1 \end{aligned} \tag{30}$$

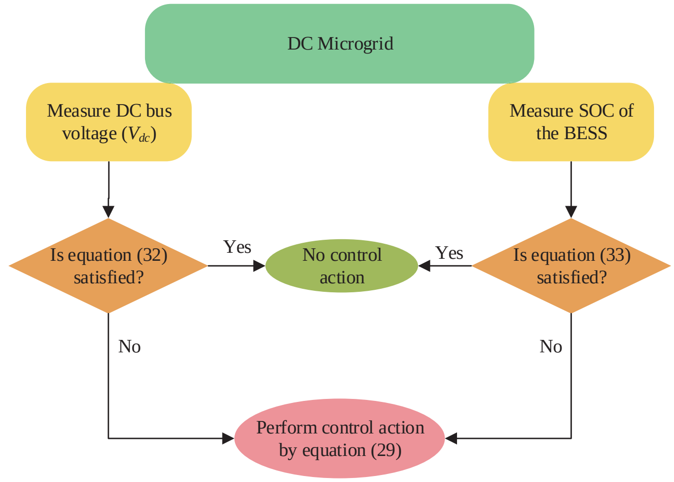

Fig. 3. Control actions by monitoring SOC of BESS and DC bus voltage

Finally, equation (28) reduce to

$$\dot{W}_3 = -k_1e_1^2-k_2e_2^2-k_3e_3^2 \tag{31}$$

From equation (31), it is obvious that the error dynamics of the system is stable as the derivative of the CLF is negative semi-definite. Therefore, the derived adaptive backstepping control law stabilizes the BESS along with the bidirectional converter. The analysis of energy state of the BESS is shown in the following section.

V. Energy State of the BESS, DC Bus Voltage and Control Actions

The controller performs its operation based on the energy level of the BESS and DC bus voltage. Thus, the energy states of BESSs and the DC bus voltage need to be continuously monitored in order to avoid over charging and discharging as well as over voltage or under voltage problems within the DC microgrid. The overall charging and discharging capability of the proposed controller along with maintaining the desired DC bus voltage will be clarified from the flowchart as shown in Fig. 3. The controller with gather information from the BESS and DC bus voltage before performing any control action. When the controller will observe that the DC bus voltage is within the specified limits and the state of charge (SOC) of the battery also satisfies a certain condition, the controller will not perform any action. The conditions for the DC bus voltage and SOC can be written as follows:

$$V_{dc_{min}} < V_{dc} \leq V_{dc_{max}} \tag{32}$$
$$SOC_{min} < SOC \leq SOC_{max} \tag{33}$$

where $V_{dc_{min}}$ is the minimum desired voltage for the DC bus, $V_{dc_{max}}$ is the maximum allowable voltage at the Dc bus, SOC_{min} is the minimum SOC of the battery, and SOC_{max} is the maximum SOC of the battery.

When the SOC of the battery will be less than the SOC_{min}, the controller will perform ist action to charge the battery until it reaches to SOC_{max}. In this condition, the BESS will be charged either from the diesel generator or from the solar PV system based on the availability. In this paper, the SOC is regulated between 30% and 80% in order to protect the battery from deep cycle discharging and overcharging. On the other hand, the battery will

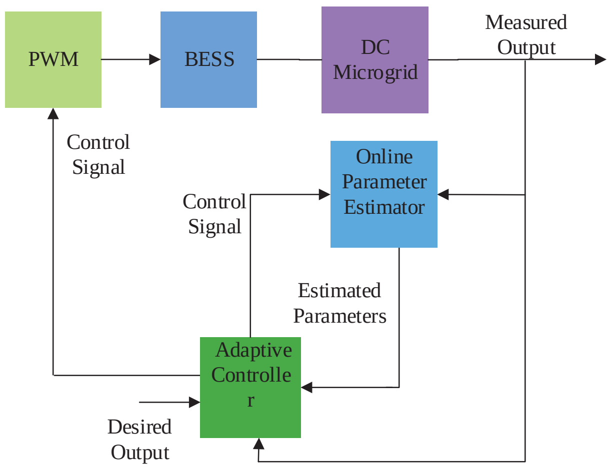

Fig. 4. Implementation block diagram of the adaptive backstepping controller for the BESS

also be charged or discharged when the DC bus voltage violets the specified limits of the Dc bus voltage as indicated by the above equation. Fig. 3 clearly reflects these situations and simulation studies are conducted in the following section to demonstrate the effectiveness of the designed controller.

VI. Simulation Results and Discussion

Simulations are conducted on a DC microgrid similar to that as presented in Fig. 1. The nominal DC bus voltage is considered as 400 V and the capacitance of the capacitor which is connected at the output of the bidirectional converter is 3000 F, the rated power of the diesel generator is 15 kW. The PV system has a maximum power rating of 10 kW with solar irradiance of 1000 W/m^2 and an operating temperature of 298 K. The maximum load demand for the DC microgrid is 10 kW. In this paper, a Lithium-ion battery is used as BESS with voltage of 110 V DC and capacity of 150 Ah with an internal resistance 0.02 Ω. The switching frequency of the converter is set to 5 kHz with a sampling frequency of 10 kHz. The implementation block diagram of the designed control scheme is shown in Fig. 4 from where it can be seen that the implementation of the controller is quite straightforward though it involves complex computation during the design process. From Fig. 4, it is clear that the online parameter estimators are used to estimate the unknown parameters where the estimation normally starts from some initial values. The estimator continuously uses the control signal and measures the desired outputs of the DC microgrid and update the parameters until the desired values are obtained. Finally, the control signal is fed to the DC-DC converter of BESS through the pulse width modulator(PWM).

For the simulation, the PV system is activated first to build the DC-link voltage and consequently the BESS and loads. To analysis the effectiveness of the designed control scheme, different operating scenarios are considered and the results are compared with a sliding mode controller as proposed in [25].

- **Case I: Power supplied by the solar PV and BESS under constant load and changing atmospheric conditions**

In this scenario, the available output power (P_{pv}) from the solar PV system is larger than the desired load demand ($P_L = 5$ kW) for a period t=0 s to t=6 S. During this period, the solar PV system is operating at the standard atomospheric conditions. i.e., the solar irradiation is 1000 W/m^2 and environmental temperature is 298 K. Thus, the solar PV system will supply excessive maximum power ($P_{pv} = 10\ kW$) for this period which can also be seen from Fig. 5 (a). The excessive power (5 kW) will be stored into the BESS after fulfilling the load demand and this is shown in Fig. 5 (c). The load power is shown in Fig. 5 (b). The corresponding DC bus voltage is shown in Fig. 6.

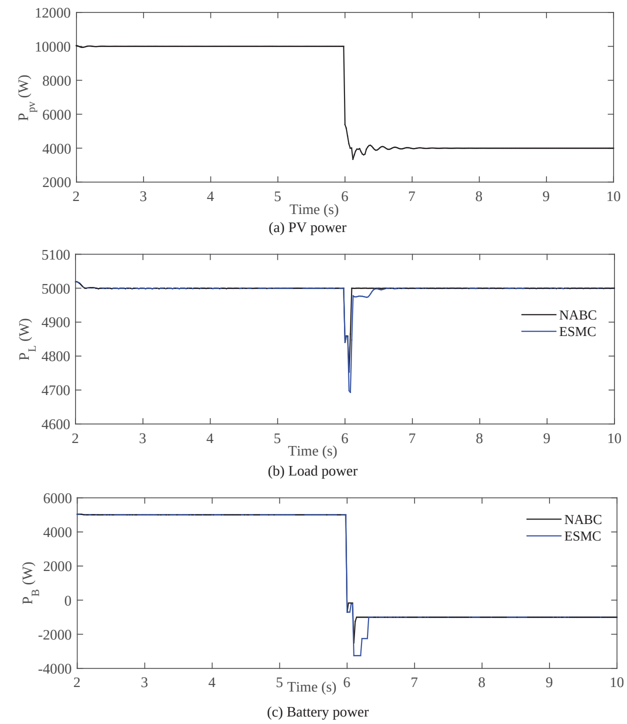

Fig. 5. Power in the DC microgrid under changing of solar irradiation while charging and discharging the BESS

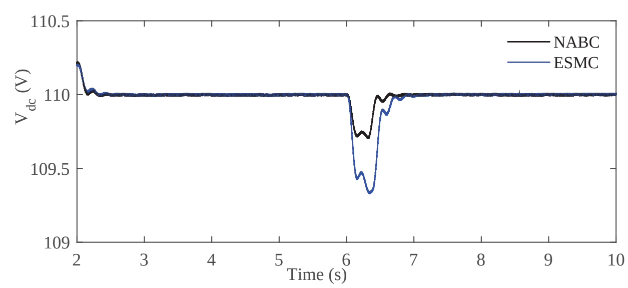

Fig. 6. DC bus voltage in the microgrid under changing of solar irradiance while charging and discharging the BESS

At t=6 s, the solar irradiance has a step change from 1000 W/m^2 to 600 W/m^2 and the solar PV system continues to run under this condition till t=10 s. During this period cell temperature is still considered as constant at 298 K. The output power of the solar PV system will now be less than the desired load demand ($P_L = 5$ kW) for such a change in the solar irradiation. In this situation, the BESS will be discharged to match the demand and maintain the desired DC bus voltage. During this condition, the changes in the power and voltage can be seen from Fig. 5 and Fig. 6, respectively. From these figures, it can be seen that there are some transient at the instant of changing the solar irradiation. However, the designed nonlinear adaptive backstepping controller (NABC) acts faster than the existing sliding mode controller

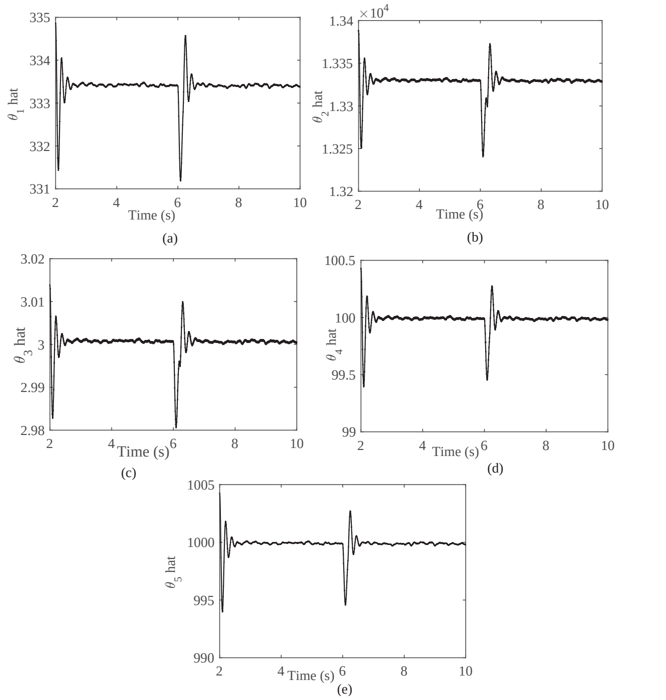

Fig. 7. Estimated parameters of the BESS with the DC-DC converter under changing of solar irradiance while charging and discharging the BESS

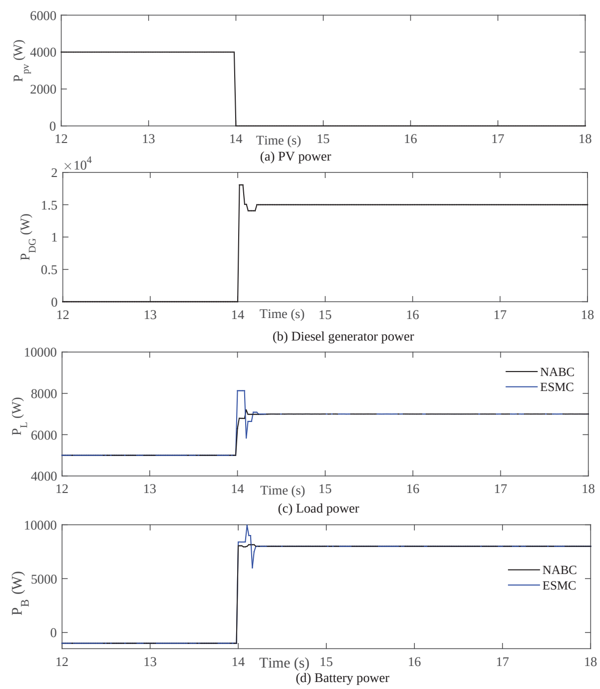

Fig. 8. Power in the microgrid under changing load demand while supplying power by the diesel generator

(ESMC) in terms of discharging the BESS and maintaining the DC bus voltage to its steady-state values. Under these conditions, the corresponding parameter estimation capability of the proposed controller is shown in Fig. 7 which indicates the steady-state values of the unknown parameters are estimated very quickly.

- **Case II: Power supplied by the solar PV, BESS, ad diesel generator while changing the loads**

This scenario is basically the continuation of the previous

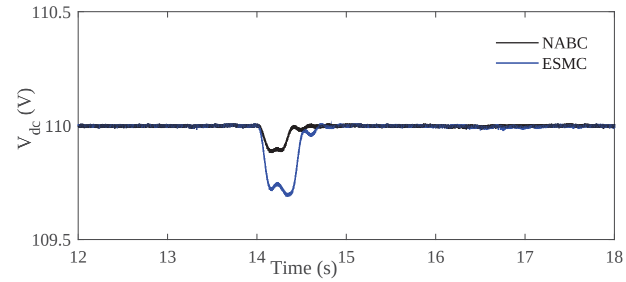

Fig. 9. DC bus voltage in the microgrid under changing load demand while supplying power by the diesel generator

scenario. In this scenario, the solar PV system continues to run with the reduced solar irradiation, i.e., with 600 W/m^2 till t=14 s. In the same time, the battery will continue to discharging and the SOC will be lower than 30% at t=14 s and in the meantime, the solar irradiation becomes zero, i.e., there is no pwer from the BESS as well as from the solar PV system. At the same instant, the load demand also increases from 5 kW to 7 kW. In this situation, the diesel generator will supply the power to the load and the BESS will also be charge from the diesel generator. The whole scenario is simulated till t=18 s and the power balancing is shown in Fig. Fig. 8 and the Dc bus voltage is shown in Fig. 9. From both Fig. 8 and Fig. 9, it can be seen that power and voltage are disturbed at t=14 s. However, the designed controller helps the microgrid to quickly recover these disturbances.

Therefore, it can be said that the designed controller has the ability to estimate the unknown parameters under changing atmospheric conditions as well as to maintain the power balancing capability under different operating scenarios.

VII. Conclusions

A nonlinear adaptive backstepping controller is designed for a BESS to maintain the overall power balance within a DC microgrid. The controller is designed by considering the parameters of BESSs and bidirectional converters as totally unknown while adapting these parameters through the adaptation laws. The overall stability of the system is analyzed through the CLFs and the negative semi-finiteness of the derivative of CLFs ensures theoretical stability of the microgrid. The maintenance of the constant DC bus voltage is considered as an indication of the power balance and the designed controller maintains a constant DC bus voltage under different operating conditions. Simulation results clearly indicate that the designed controller is robust against different practical operating scenarios and unknown parameters of the BESS with a bidirectional converter. Future work will be devoted to design a cooperative controller for all components which will be delivering power into DC microgrids.

References

[1] H. Kakigano, Y. Miura, and T. Ise, "Low-voltage bipolar-type DC microgrid for super high quality distribution," *IEEE Trans. on Power Electronics*, vol. 25, no. 12, pp. 3066–3075, December 2010.

[2] B. Liu, F. Zhuo, Y. Zhu, and H. Yi, "System operation and energy management of a renewable energy-based DC microgrid for high penetration depth application," *IEEE Trans. on Smart Grid*, vol. 6, no. 3, pp. 1147–1155, May 2015.

[3] I. Tank and S. Mali, "Renewable based DC microgrid with energy management system," *IEEE Int. Conf. on Signal Processing, Informatics, Communication and Energy Systems*, pp. 1–5, 2015.

[4] S. Morozumi, S. Kikuchi, and Y. Chiba, “Distribution technology development and demonstration projects in Japan,” *IEEE Power and Energy Society General Meeting-Conversion and Delivery of Electrical Energy*, July 2008.

[5] F. A. Mohamed and H. N. Koivo, “System modelling and online optimal management of microgrid using mesh adaptive direct search,” *Int. Journal of Electrical Power and Energy Systems*, vol. 32, no. 5, pp. 398–407, 2010.

[6] V. Nasirian, A. Davoudi, F. L. Lewis, and J. M. Guerrero, “Distributed adaptive droop control for DC distribution systems,” *IEEE Trans. on Energy Conversion*, vol. 29, no. 4, pp. 944–956, December 2014.

[7] C. L. Chen, Y. Wang, J. S. Lai, Y. S. Lee, and D. Martin, “Design of parallel inverters for smooth mode transfer microgrid applications,” *IEEE Trans. on Power Electronics*, vol. 25, no. 1, pp. 6–15, January 2010.

[8] I. J. Balaguer, Q. Lei, S. Yang, U. Supatti, and F. Z. Peng, “Control for grid-connected and intentional islanding operations of distributed power generation,” *IEEE Trans. on Industrial Electronics*, vol. 58, no. 1, pp. 147–157, January 2011.

[9] A. Llaria, O. Curea, J. Jimenez, and H. Camlong, “Survey on microgrids: unplanned islanding and related inverter control techniques,” *Renewable Energy*, vol. 36, pp. 2052–2061, 2011.

[10] A. Radwan and Y.-R. Mohamed, “Stabilization of medium-frequency modes in isolated microgrid supplying direct online induction motor loads,” *IEEE Trans. on Smart Grid*, vol. 5, no. 1, pp. 358–370, January 2014.

[11] C. Cho, J.-H. Jeon, J.-Y. Kim, S. Kwon, K. Park, and S. Kim, “Active synchronizing control of a microgrid,” *IEEE Trans. on Power Electronics*, vol. 26, no. 12, pp. 3707–3719, December 2011.

[12] M. A. Mahmud, M. J. Hossain, H. R. Pota, and A. M. T. Oo, “Robust nonlinear distributed controller design for active and reactive power sharing in islanded microgrids,” *IEEE Trans. on Energy Conversion*, vol. 29, no. 4, pp. 893–903, December 2014.

[13] H. Kakigano, M. Nomura, and T. Ise, “Loss evaluation of dc distribution for residential houses compared with ac system,” *Int. Power Electronics Conference-ECCE Asia*, pp. 480–486, 2010.

[14] T. K. Roy, M. A. Mahmud, M. J. Hossain, and A. M. T. Oo, “Nonlinear backstepping controller design for sharing active and reactive power in three-phase grid-connected photovoltaic systems,” *Australasian Universities Power Engineering Conference*, pp. 1–6, 2015.

[15] M. A. Mahmud, M. J. Hossain, H. R. Pota, and N. K. Roy, “Nonlinear distributed controller design for maintaining power banlance in islanded microgrids,” *PES General Meeting, Conference and Exposition*, pp. 1–5, 2014.

[16] N. Eghtedarpour and E. Farjah, “Control strategy for distributed integration of photovoltaic and energy stroage systems in DC microgrid,” *Renewable Energy*, vol. 45, pp. 96–110, 2012.

[17] S. X. Chen and H. B. Gooi, “Jump and shift method for multi-objective optimization,” *IEEE Trans. on Industrial Electronics*, vol. 58, no. 10, pp. 4538–4548, October 2011.

[18] D. Chen and L. Xu, “Autonomous DC voltage control of a DC microgrid with multiple slack terminals,” *IEEE Trans. on Power System*, vol. 27, no. 4, pp. 1897–1905, November 2012.

[19] Y. Mohamed and E. F. El-Saadany, “Adaptive decentralized droop controller to preserve power sharing stability of paralleled inverters in distributed generation microgrids,” *IEEE Trans. on Power Electronics*, vol. 23, no. 6, pp. 2806–2816, November 2008.

[20] R. A. F. Ferreira, H. A. C. Braga, A. A. Ferreira, and P. G. Barbosa, “Analysis of voltage droop control method for dc microgrids with simulink: modelling and simulation,” *in Proc. of the 10th IEEE/IAS Int. Conf. on Industry Applications*, pp. 1–6, 2012.

[21] J. M. Guerrero, J. C. Vasquez, J. Matas, L. G. de Vicuna, and M. Castilla, “Hierarchical control of droop-controlled AC and DC microgridsa general approach toward standardization,” *IEEE Trans. on Industrial Electronics*, vol. 58, no. 1, pp. 158–172, January 2011.

[22] N. L. Diaz, T. Dragievi, J. C. Vasquez, and J. M. Guerrero, “Intelligent distributed generation and storage units for DC microgridsa new concept on cooperative control without communications beyond droop control,” *IEEE Trans. on Smart Grid*, vol. 5, no. 5, pp. 2476–2485, September 2014.

[23] H. Kakigano, Y. Miura, and T. Ise, “Distribution voltage control for DC microgrids using fuzzy control and gain-scheduling technique,” *IEEE Trans. on Power Electronics*, vol. 28, no. 5, pp. 2246–2258, May 2013.

[24] A. Tahim, D. Pagano, and E. Ponce, “Nonlinear control of DC-DC bidirectional converters in stand-alone DC microgrids,” *in Proc. of the 51st Annual Conference on Decision and Control*, pp. 3068–3073, 2012.

[25] A. Agarwal, K. Deekshitha, S. Singh, and D. Fulwani, “Sliding mode control of a bidirectional DC/DC converter with constant power load,” *IEEE 1st Int. Conf.e on DC Microgrids*, pp. 287–292, 2015.

[26] D. Jenkins, J. Fletcher, and D. Kane, “Lifetime prediction and sizing of lead-acid batteries for microgeneration storage applications,” *IET Renewable Power Generation*, vol. 2, no. 3, pp. 191–200, September 2008.

[27] F. A. Mohamed and H. N. Koivo, “Online management of microgrid with battery storage using multiobjective optimization,” *in Proc. of the Int. Conf. on Power Engineering, Energy and Electrical Drives*, pp. 231–236, 2007.

[28] H. E. Fadil, F. Giri, O. E. Magueri, and F. Chaoui, “Control of DCDC power converters in the presence of coil magnetic saturation,” *Contr. Eng. Pract.*, vol. 17, no. 7, pp. 849–862, 2009.